

## **Interannual and Interdecadal Variations of the East Asian Summer Monsoon and Tropical Pacific SSTs.**

### **Part 1: Roles of the Subtropical Ridge**

C.-P. Chang, Yongsheng Zhang and Tim Li

Department of Meteorology, Naval Postgraduate School, Monterey, CA 93943

#### **Abstract**

The interannual relationship between the East Asian summer monsoon and the tropical Pacific sea-surface temperatures (SST) is studied using rainfall data in the Yangtze River Valley and the NCEP reanalysis for 1951-1996. The data sets are also partitioned into two periods, 1951-77 and 1978-96, to study the interdecadal variations of this relationship.

A wet summer monsoon is preceded by a warm equatorial eastern Pacific in the previous winter and followed by a cold equatorial eastern Pacific in the following fall. This relationship involves primarily the rainfall during the pre-Meiyu/Meiyu season (May-June) but not the post-Meiyu season (July-August). In a wet monsoon year, the western North Pacific subtropical ridge is stronger as a result of positive feedback that involves the anomalous Hadley and Walker circulations, an atmospheric Rossby wave response to the western Pacific complementary cooling, and the evaporation-wind feedback. This ridge extends farther to the west from the previous winter to the following fall, resulting in an 850 hPa anomalous anticyclone near the southeast coast of China. This anticyclone (1) blocks the pre-Meiyu and Meiyu fronts from moving southward thereby extending the time that the fronts produce stationary rainfall, (2) enhances the pressure gradient to its northwest resulting in a more intense front, and (3) induces anomalous warming of the South China Sea surface through increased downwelling which leads to a higher moisture supply to the rain area. A positive feedback from the strong monsoon rainfall also appears to occur, leading to an intensified anomalous anticyclone near the monsoon region. This SST-subtropical ridge-monsoon rainfall relationship is observed in both the interannual time scale within each interdecadal period and in the interdecadal scale.

The SST anomalies (SSTA) change sign in northern spring and resemble a tropospheric biennial oscillation (TBO) pattern during the first interdecadal period (1951-77). In the second interdecadal period (1978-96) the sign change occurs in northern fall and the TBO pattern in the equatorial eastern Pacific SST is replaced by longer time scales. This interdecadal variation of the monsoon-SST relationship results from the interdecadal change of the background state of the coupled ocean-atmosphere system. This difference gives rise to the different degrees of importance of the feedback from the anomalous circulations near the monsoon region to the equatorial eastern Pacific.

In a wet monsoon year, the anomalous easterly winds south of the monsoon-enhanced anomalous anticyclone start to propagate slowly eastward towards the eastern Pacific in May and June, apparently as a result of an atmosphere-ocean coupled wave motion. These anomalous easterlies carry with them a cooling effect on the ocean surface. In 1951-77 this effect is insignificant as the equatorial eastern Pacific SSTA already change from warm to cold in northern spring, probably as a result of negative feedback processes discussed in ENSO mechanisms. In 1978-96 the equatorial eastern Pacific has a warmer mean SST. A stronger positive feedback between SSTA and the Walker circulation during a warm phase tends to keep the SSTA warm until northern fall, when the eastward-propagating anomalous easterly winds reach the eastern Pacific and reverse the SSTA.

## 1. Introduction

The East Asian summer monsoon has complex space and time structures that are distinct from the South Asian (Indian) monsoon. It covers both the tropics and midlatitudes and its rainfall season consists of staged progression of zonally oriented rain belts which contains mixed tropical and baroclinic properties (Chen and Chang, 1980). On average, the onset occurs in early to mid-May when heavy convective rainfall develops along the pre-Meiyu front that extends from the southern coast of China into the western Pacific south of Japan (Johnson et al. 1993). This is normally followed by the northward movement of the elongated rain belt to the Yangtze River Valley and southern Japan after mid-June, which is referred to as Meiyu in China and Baiu in Japan. In July the climatological rain belt moves northward to northern China, Yellow Sea, and southern Japan Sea. In August, the monsoon begins to withdraw southward (Tao and Chen, 1987; Ding, 1992, 1994). This climatological intraseasonal space-time structure, however, experiences large interannual variations so that a flood condition may result from heavier-than-normal rainfall during the normal rain period or from sustained rainfall outside of the normal period or both.

The severe flood and drought events that occurred frequently during the summer monsoon have motivated many climate scientists in the region to look for predictors. In particular, the relationship between tropical sea-surface temperatures (SST) and the East Asian monsoon has been the subject of many studies in the past decade. Chinese researchers have used northern winter El Nino<sup>1</sup> or northern spring La Nina<sup>2</sup> events as a predictors for floods over China during the summer monsoon. While the overall result of the predictions has been successful in recent years, the details of the relationship appear to be complex. For example, Huang and Wu (1989), using data from 1950-1980, found that the developing stage of a warm ENSO event coincides with drought in southern and northern China and flood in central China – in the Yangtze River Valley and Huaihe Valley. The relationship appears reversed in the summer after the ENSO begins to decay. Similar results were also obtained by Liu and Ding (1992). In another study using OLR and 500 hPa geopotential height data during 1978-1989, Huang and Sun (1992) shifted their attention away from the equatorial eastern Pacific SST, and found that the China monsoon rainfall anomalies are simultaneously correlated with the convection activity around the Philippines. With an atmospheric GCM simulation they found this convection activity to be largely driven by the western Pacific warm pool SST. Through a teleconnection pattern, a warmer western Pacific and stronger Philippines convection shift the western Pacific subtropical high northward and cause a drought in the Yangtze River Valley and floods in southern and northern China.

Shen and Lau (1995), using 1956-1985 data, found a strong biennial signal in the correlations between East Asian summer monsoon (as represented by rainfall over China) and the tropical SST. Their lag correlations show that a wet East Asian summer monsoon is preceded by warm eastern and central equatorial Pacific and Indian Ocean SST anomalies (SSTA) in the previous winter (Fig. 1, Shen and Lau's Fig. 9). These SSTA decay and switch sign in northern spring, leading to cool anomalies after the monsoon rain starts. The cooling continues through northern fall and peaks in the following winter. Thus the tropical SST and the East Asian summer monsoon are related in a system resembling the tropical biennial oscillation (TBO) described by Meehl (1987, 1997) and others. There is also a correlation between the monsoon and the tropical western Pacific SST which is opposite to that of the eastern Pacific

---

<sup>1</sup> Forecast Bulletin for the South China Sea Monsoon Experiment, National Climate Center of China, Beijing, 1 April 1998

<sup>2</sup> Chao, Jiping, "1997/1998 El Nino-La Nina", China Science News, Chinese Academy of Sciences, Beijing, 25 September 1998.

SST. Overall, the TBO relationship between the East Asian summer monsoon and the tropical SST resembles a similar relationship for the Indian monsoon (e.g., Yasunari 1990; Lau and Yang 1996; Webster et al. 1998). In this TBO relationship the summer monsoon in China will be strong after an El Niño-like condition in the preceding winter. The SSTA change sign in northern spring just before this strong monsoon starts, and in the following year a weak summer monsoon will follow a La Niña-like condition in the winter. Shen and Lau (1995) argued that this biennial relationship in the SST-East Asian monsoon interaction is more robust than the one on the ENSO time scale.

These studies raised some important questions about the relationship between the East Asian summer monsoon and the tropical SSTs. What are the processes involved in the correlation between the Pacific SST and the East Asian summer monsoon? The TBO relationship holds if El Niño-type and La Niña-type conditions alternate from one year to the next. Is a similar relationship present across different interannual time scales? In particular, the tropical eastern Pacific SST and circulation regimes after the middle 1970 have undergone noticeable changes (e.g., Trenberth and Hurrell 1994, Wang 1995, Kachi and Nitta 1997). There have been apparent increases of warm events compared to cold event and a lowering of the sea-level pressure in the tropical Pacific. This change may due to a general warming of mean SSTs (Trenberth and Hoar, 1996; Meehl and Washington 1996) or the occurrence of an in-phase relationship between the decadal, long-term trend and interannual time scales (Lau and Weng, 1999).

This variation likely affects the relationship between the SSTA and the East Asian summer monsoon rainfall. For example, Nitta and Hu (1996) and Weng et al. (1999) found that certain EOF components of rainfall over China underwent a significant shift in the late 1970s, and Tanaka (1997) found that the maximum negative correlation between NINO3 SST and July rainfall over eastern China and Japan as a whole increased after 1978. Thus, how these interdecadal changes may affect the interannual East Asian summer monsoon-tropical SST relationship will be an important focus of this study.

Another important question arises from the different meridional structures of the interannual variations of the East Asian summer monsoon reported by Huang and Wu (1989), Liu and Ding (1992), Huang and Sun (1992), Tian and Yasunari (1992), and Shen and Lau (1995). These results include a variety of phase relationships between central and southeastern China that are inconsistent with each other.

To answer these questions, Chinese rainfall records of 1951-1996 are used to study the relationships between the interannual variability of the East Asian summer monsoon rainfall and tropical SSTs. Since the Meiyu rainfall is one of the most important indicators of the East Asian summer monsoon, this paper (Part 1) will concentrate on the results analyzed from the summer monsoon rainfall in the vicinity of the Yangtze River Valley in central China. This is the region where a correlation with El Niño conditions has been reported in nearly all the previous studies. In Part 2 we will discuss the results concerning the variable structure of the tropical Pacific SST - East Asian summer monsoon relationship when both central and southeastern China are considered together.

## **2. Data and Methodology**

The summer monsoon rainfall over China is represented by two area-averaged precipitation indices during May-August (MJJA): the middle and lower Yangtze River Valley (YRV, 27°-34°N, 110°-125°E), where mean maximum rainfall during the mature monsoon (Meiyu) occurs; and the southeastern coastal area of China (SEC, 20°-27°N, 110°-125°E), which is the favored location of the maximum rainfall belt during the early season (pre-Meiyu). We chose this approach rather than principal components such as EOFs used in many previous

studies, because the latter may be sensitive to the choice of the spatial domain and the data period (Weng et al. 1999).

We computed the interannual correlations between all Indian summer rainfall and summer rainfall over these two regions as well as northern China for the 46-year period (not shown). Only northern China shows a significant (and positive) correlation with the Indian rainfall, which is in agreement with the results of Yatagai and Yasunari (1995). However, the northern China summer rainfall is much less than either the YRV or the SEC and will not be studied here. Fig. 2 shows the two regions and the rainfall stations used, superimposed with the climatological MJJA rainfall pattern. The stations are selected because their records are available every year between 1951-1996 from the China Meteorological Administration, and are rarely missing (never more than a few days in a month). The SSTA, over the tropical region covering the Pacific and Indian Oceans between 21°S and 37°N, are composited from the Reynolds SST data set according to the annual monsoon rainfall anomalies.

Fig. 3 shows that the correlation between SEC and YRV rainfalls is highly positive in fall, winter and early spring, reflecting the fact that practically all weather systems are developed from higher latitudes. The correlation becomes much lower in late spring and summer due to tropical influences, with April to June positive and July - August negative. This contrast motivates us to also examine the pre-Meiyu/Meiyu (May-June, or MJ) and post-Meiyu (July-August, or JA) seasons separately. The MJ season includes the pre-Meiyu period for SEC in mid-May to mid-June and the Meiyu period for YRV in late June. These are the peaks of their respective annual rainfall cycles, and the rainfall is produced along pre-Meiyu or Meiyu fronts that move southward into their quasi-stationary locations during summer. July and August are the period of maximum tropical influences, particularly in SEC. In these two months weather systems originating from the tropics have increased influences on the production or impediment of heavy rainfall.

For both regions the anomalies of the seasonal monsoon rainfall over the 46 years are composited according to five categories that are defined by a ranking of the rainfall amount: very wet (category 1, the wettest seven years), wet (category 2, the next nine years), normal (category 3, the middle 14 years), dry (category 4, the next nine years) and very dry (category 5, the driest seven years). The categorizations are listed in Table 1 under the "ALL" column. The relationship with the composite SSTA from December of the year before the monsoon (Year -1) to November of the monsoon year (Year 0), are plotted on a map according to the following symbols:

**+** : SSTA positive for both very wet and wet, negative for both very dry and dry.

**+**: SSTA positive for very wet and negative for very dry. Either very wet in-phase with wet or very dry in-phase with dry but not both.

**-**: SSTA negative for both very wet and wet, positive for both very dry and dry.

**-**: SSTA negative for very wet and positive for very dry. Either very wet in-phase with wet or very dry in-phase with dry but not both.

Significant long-term changes in the distributions of tropical Pacific SST and upper tropospheric velocity potential occurred around 1976-1978 (e.g., Nitta and Yamada 1989, Wang 1995). A sudden shift in the rainfall anomaly of some components of rainfall over China around this period was also reported (e.g., Nitta and Hu 1996, Weng et al. 1999). To consider the possible effects of these interdecadal changes, we use Wang's (1995) description of the SST variation and divided the data set into two periods, 1951-77 (interdecadal period 1, or ID1) and 1978-96 (interdecadal period 2, or ID2). This division also corresponds to that used by Weng et

al. (1999). The rationale of this division may be examined by computing the correlations between the total May-June YRV and SEC rainfall and March-May Nino 3 SST for all 11-year periods (not shown) in the data set. The correlations are consistently negative for all periods centered in a year before 1978 and near zero or positive for all periods centered after 1977.

Because the number of years within each interdecadal period is smaller, we divide them evenly into three rainfall categories (wet, normal, dry). These categorizations are also shown in Table 1. It may be noticed that the category of a given year and season never differ by more than one level among the ALL, ID1 and ID2 columns.

The 850 hPa wind and 500 hPa geopotential height available from NCEP reanalysis for the entire 46 years are also used. The wind anomalies are computed by subtracting the average of all dry cases (both very dry and dry) from the average of all wet (both very wet and wet) cases. These composites are referred to as “wet-minus-dry” maps. The height anomalies are not explicitly computed, rather, the 5860 m and 5880 m contours for both the wet and dry composites are plotted together to indicate the location and strength differences of the western Pacific subtropical ridge. The 5860 m contour is often the outermost closed contour, at 20 m intervals, that defines the subtropical ridge during northern winter and spring.

### **3. Composite relative to Yangtze River Valley rainfall**

#### ***a) SST anomalies***

Fig. 4 shows the monthly SSTA composite for YRV, starting from the December prior to the summer rain season (DEC-1) and ending with the November following the rain season (NOV0). Here it is seen that a wet summer season is preceded by warm SSTA in the equatorial eastern Pacific and the Indian Ocean that can be traced back to the preceding winter. This pattern weakens somewhat in May, but the SSTA in both regions remain warm. A conspicuous feature in May is the first development of prolonged warm SSTA in the South China Sea that expands to the westernmost Pacific east of the Philippines. This warm pattern persists through October. The South China Sea SSTA reverse sign in November. Beginning in June the northeastern tropical Pacific shows a cooling trend. The cooling area extends southwestward towards the equator near the dateline and by September it forms a northeast-southwest oriented cool tongue extending from Baja California to the equatorial central Pacific. In October and November the cool area expands eastward along the equator, resulting in a pattern that seems to be the opposite of the December distribution one year before. The Pacific and Indian Ocean SST changes are consistent with the lag-correlation results between monsoon and equatorial SST indexes reported by Shen and Lau (1995), and also resembles Yasunari's (1990) correlation results for the Indian monsoon. In these results a strong monsoon rainfall is preceded by warm equatorial eastern Pacific and Indian ocean SSTA in the preceding northern winter and followed by cool anomalies in the next winter. Thus, it appears that the YRV and South Indian monsoon rainfall share the gross characteristics of a tropospheric biennial oscillation (TBO, see Meehl 1987,1994) in terms of their relationship with the equatorial eastern Pacific and Indian Ocean SST.

To investigate possible interdecadal variations in monsoon-SST relationships, the YRV rainfall is separated into the first interdecadal period, 1951-1977 (ID1), and the second interdecadal period, 1978-1996 (ID2). For ID1 there are nine years in each category, for ID2 there are six years each in the dry and wet categories and seven years normal (Table 1). The SST composites for the two periods are shown in Figs. 5a and 5b, respectively. Here a + sign indicates that the composite SSTA are positive for wet and negative for dry, and a – sign indicates the reverse. Wet years in both periods are preceded in the previous winter by warm SSTA in the equatorial eastern Pacific and the Indian Ocean, but by May the patterns of the two periods are nearly opposite. In ID1 a reverse (cooling) of the equatorial eastern Pacific and

Indian Ocean SSTA occurs in northern spring before the wet YRV rainfall, but in ID2 the reversal does not occur until northern fall after the wet YRV summer. This difference results in very weak SSTA signals in the equatorial eastern Pacific and Indian Ocean during northern summer for the 46-year composite (Fig. 4). A similar difference between the two periods but with an opposite SSTA tendency also appears in the tropical western Pacific.

The contrast between the two interdecadal periods in the equatorial eastern Pacific SSTA evolution is summarized in Fig. 6. Here the normalized wet-minus-dry area-averaged SSTA over  $5^{\circ}\text{S}$ - $5^{\circ}\text{N}$ ,  $105^{\circ}\text{W}$ - $85^{\circ}\text{W}$  are plotted relative to the YRV MJJA rain season, from the October before the rain season (OCT-1) to the second December after the rain season (DEC+1). For both interdecadal periods, the equatorial eastern Pacific SSTA are warm in the fall and winter prior to a wet season and cool in the fall and winter immediately following a wet season. The change of sign occurs in early spring before the summer rain season for ID1, similar to Shen and Lau's (1995) result (Fig. 1). But in ID2 the change of sign occurs in early fall after the rain season. Furthermore, in ID1 the SSTA turn to warm in the ensuing spring, indicating a TBO signal. However, for ID2 the negative SSTA, although decreased in magnitude in the ensuing spring, become colder in the summer and appear to reach coldest value in the following fall. If the SSTA-YRV rainfall relationship in the first year of the diagram holds, this means the YRV becomes a drought in year +2 rather than +1, and the TBO cycle is broken. These interdecadal differences are nearly reproducible relative to the YRV MJ rainfall but not relative to the JA rainfall.

The mean equatorial eastern Pacific SST in ID2 is warmer than ID1. The differences in the SSTA-YRV relationship between the two interdecadal periods during northern summer shown in Figs. 5a-b are the result of computing the monthly means within each interdecadal period. Thus, while the relationship during the summer rain season is opposite between the two periods with respect to their own respective period-means, the relationship with respect to the 46-year mean may or may not be opposite. To examine this question, we use the five-category method (Fig. 4) to composite the SSTA with respect to the 46-year mean for the two interdecadal periods separately. The results of these composites (not shown) will be called "extra-period" correlations to differentiate them with the "intra-period" correlations produced with respect to the mean of each interdecadal period. In general, the areas covered by the extra-period correlation signals are smaller, although the overall patterns are similar to the intra-period correlations shown in Figs. 5a and 5b. Thus, the difference in the intra-period SSTA-YRV correlations between the two interdecadal periods from northern spring to northern fall exists for the extra-period correlations as well.

In spite of the opposite signs in the equatorial eastern Pacific SSTA between the two interdecadal periods, during June, July and August the SSTA in the South China Sea are in-phase with the YRV rainfall anomaly in both interdecadal periods. This is readily visible in Figs 5a-b. This relationship is also robust with respect to the extra-period relationship. Another area where strong signals appear is in the Indian Ocean, where the phase is positive from May to September.

When the YRV rainfall anomalies are divided into pre-Meiyu/Meiyu (May-June) and post-Meiyu (July-August) season composites, the SSTA relationships change again. The interannual trend of the MJ season results are basically similar to the MJJA composites with a wet rainfall preceded by warm equatorial eastern Pacific and Indian Ocean in the winter and cool SSTA there afterwards. But in the JA composite the equatorial eastern Pacific SSTA remain positive throughout the wet year; therefore a coherent TBO signal cannot be inferred.

The patterns of all the different composites of equatorial eastern Pacific SSTA relative to the YRV rainfall anomalies are schematically outlined in Table 2, where a + sign indicates in-

phase, a - sign indicates out-of-phase, and 0 indicates no clear relationship between SSTA and the YRV rainfall anomalies. Whenever there is a division into the two interdecadal periods, two signs are shown, with the first being the intra-period and the second the extra-period result. The table may be summarized as follows:

1) A wet YRV summer occurs after warm eastern Pacific SSTA in the preceding northern winter and is followed by cold eastern Pacific SSTA in the following fall. A significant interdecadal variation exists for the timing of this SSTA sign change. In ID1 (1951-77) the sign change occurs in late winter-early spring before the Meiyu. In ID2 (1978-96) the sign change occurs in fall after the rain season, with an intra-period sign change in August and an extra-period sign change in November.

2) For the pre-Meiyu/Meiyu season (May-June) YRV, the relationship with the equatorial eastern Pacific SSTA exhibits a TBO-type pattern, with warm SSTA in the northern winter before a wet season and cool SSTA in the northern fall (and winter) afterwards.

3) For the post-Meiyu season (July-August), neither a TBO pattern nor a strong interdecadal variation is found. For ID1, positive SSTA tend to occur throughout the year of a wet season. For ID2 positive SSTA tend to occur during and after a wet season, with the months prior to the rainfall season showing almost no signals.

Table 3 outlines the composites of South China Sea SSTA relative to the YRV rainfall anomalies. Here the most consistent feature is a warm South China Sea in the summer of a wet season. The signal is particularly strong in June, which is the mean annual cycle rainfall peak for YRV. This warm SSTA tendency exists for both intra- and extra-period correlations. So while the eastern Pacific SSTA have a lead-lag relationship with the YRV rain anomalies, the South China Sea SSTA show mainly a concurrent, positive correlation.

### ***b) Wind and height anomalies***

The wind and height anomaly composites are constructed by computing the difference between the wet- and dry-year averages<sup>3</sup>. Fig. 7 shows the monthly YRV MJJA wet-minus-dry 850 hPa wind distribution, from March to October, for the 46-year data. In general, the equatorial wind characteristics are consistent with the tropical SST-YRV rainfall relationship shown in Fig. 4. For example, in March the central and eastern Pacific shows a westerly wind anomaly for a wet season, which corresponds to warm SSTA indicated by Fig. 4. In October the wind anomaly in the central and eastern Pacific turns easterly, which corresponds to cold SSTA indicated by Fig. 4.

A conspicuous feature during summer is an anomalous anticyclone cell near the southeast coast of China, which can be seen every month from May to August. The cell is slightly east-west elongated and can be easily identified by westerly anomalies in the East China Sea to its north and easterly anomalies in the South China Sea and Philippine Sea to its south. This anomalous cell indicates that the western end of the western Pacific subtropical ridge is stronger than normal. Since the Meiyu rainfall is mostly produced from Meiyu fronts that developed after midlatitude baroclinic systems have moved into southeastern China (Chang and Chen 1995; Chang et al. 1998), the immediate effect of the anomalous anticyclone cell is a tendency to block the front from moving into the southeastern coastal (SEC) region. This increases the time the Meiyu front stays in YRV. Furthermore, the strengthened subtropical ridge will lead to a higher pressure gradient to its northwest, resulting in a more intense Meiyu front. Both of these effects will favor a wet season.

---

<sup>3</sup> In the case of the 46-year composite, all categories of wet years and dry years are used.

The development of the anomalous anticyclone cell in the 850 hPa wind field during a wet summer monsoon indicates the intensification and westward extension of the northwestern Pacific subtropical ridge. The variation of this subtropical ridge is examined by compositing the 500 hPa geopotential height. Fig. 8 shows the month-to-month evolution of the 46-year composite 5860 m and 5880 m contours relative to both the wet and dry all-summer (MJJA) rainfall. It can be noticed immediately that from the preceding winter until September the wet-composite subtropical ridge covers a larger area in the western Pacific than the dry composite. The wet-composite ridge is also stronger. From January to April the western end of this ridge extends progressively westward. In May it begins to retreat but the meridional extent of the ridge expands to cover a wider latitudinal band of the South China Sea and the western Pacific. This is also the time it begins to develop to the east and connect with the eastern Pacific subtropical ridge. The ridge strength reaches maximum in June and July, and remains stronger than the preceding winter and spring through the rest of the year.

From December through June the more westward extension of the 500 hPa ridge for the wet composite directly affects the South China Sea. The 5860 m contour also continuously moves northward, reaching the southern China coast in May and covering a part of the southeastern coastal area and the East China Sea between June and September. The influence of this strengthened ridge in southeastern China can be clearly identified by the corresponding wet-minus-dry composite of the 500 hPa height (Fig. 9). Beginning from February and through August, a large part of Asia has a positive height anomaly for the wet composite. The effect of the stronger subtropical ridge is manifested by a positive height anomaly center near Taiwan during the May-to-August rain season. This height anomaly center would support the low level anomalous anticyclone center and favor excess rainfall in the YRV through the three effects discussed earlier. Another notable feature in Fig. 9 is an anomalous trough to the north and northeast of the anomalous Taiwan high during the summer rain season. This trough simply reflects the fact that the baroclinic system responsible for the excess East Asian monsoon rainfall is stronger, which is expected from the effects of the anomalous anticyclone. In Fig. 9 the anomalous trough seems traceable backwards to February when it is over northeastern China and the North Pacific. However, its potential as a predictor of the YRV rainfall is doubtful since there is strong interdecadal variation between ID1 and ID2 (not shown).

Figs. 10a and 10b show the 500 hPa 5860 m and 5880 m contours composited according to the MJ YRV rainfall from March to June, for the two interdecadal periods. Most of the general characteristics of the all-summer composite (Fig. 8) can be seen for both periods, including the more westward extension and stronger strength of the wet-composite subtropical ridge, and a northward progression of the 5860 m contour so that the wet-composite ridge projects a larger influence on the northern South China Sea and the southeast coast of China during the rain season (in this case May and June). Figs. 10a-b show a notable interdecadal variation, in that the subtropical ridge is significantly stronger in ID2 than in ID1 for both the wet and dry composites. Since the mean SST in ID2 is a higher than in ID1, this interdecadal difference in the strength of the subtropical ridge indicates a stronger ridge development during the warmer SST period (ID2). This result indicates that the relationship between the subtropical ridge and the YRV May-June rainfall is both intra-period and extra-period in the two interdecadal periods. It also implies that the eastern Pacific SST-subtropical ridge-East Asian monsoon relationship prevails on both interannual and interdecadal time scales.

#### **4. Discussion**

It has been shown that a wet YRV monsoon is associated with a strong western Pacific subtropical ridge which occurs after warm eastern Pacific SSTA during the preceding winter. The subsidence in the ridge area may be modulated by anomalous convection associated with

the eastern Pacific SSTA through Hadley and Walker circulations (Wang 1995, Li 1997). Furthermore, the convection associated with the warm eastern Pacific SSTA may cause a complementary cooling in the western Pacific through atmospheric Rossby wave responses and through the evaporation-wind feedback (Wang et al. 2000). The Hadley-Walker circulation induced subtropical high may further interact with the underlying cold SSTA through a positive feedback mechanism (Wang et al. 2000) to maintain its strength. The persistence of this strong subtropical ridge leads to an 850 hPa anomalous anticyclone cell that blocks the southward progression of the Meiyu front as well as enhances its strength, leading to increased rainfall during the monsoon season.

The anomalous anticyclone cell may also help the concurrent development of warm SSTA in the South China Sea. Chu and Chang (1997) and Chu et al. (1997) showed that, because of the large depth of the South China Sea, Ekman-induced downwelling driven by the seasonal migration of the surface subtropical high is responsible for the warming of the upper layer of the South China Sea. An anticyclonic surface wind anomaly will therefore also lead to a higher SSTA. In addition, the anticyclonic anomaly also favors radiative warming of the sea surface during summer. The higher SST tends to lead to more evaporation, but the anomalous wind over the South China Sea itself is rather modest, about 1 m/s or less (Fig. 7), so additional evaporative cooling due to the anticyclonic anomaly may not be significant. The resultant warm South China Sea surface provides increased moisture transport into the YRV along the western side of the anomalous anticyclone cell, where the southwesterly wind is also enhanced. This gives a third effect to favor a wet season.

Fig. 7 shows that there is a sequence of events through the year that can be associated with the development of this anticyclonic anomaly cell. An anticyclonic anomaly cell in the western Pacific can be traced back to January (not shown), when an anticyclone circulation exists between equator and 15°N southeast of Philippines. The circulation is delineated mainly by strong anomalous easterlies in the equatorial ocean immediately east of the maritime continent. It weakens considerably in February (not shown) and March, when the anticyclonic area expands eastward to cover most of the tropical Northwest Pacific. In April the ridge is enhanced by increased wind to its southeast and south, and an expansion of its northern fringe to around 30°N. By May the anomalous anticyclone penetrated into the South China Sea with its strongest part shifting to the western portion, resulting in the configuration that favors a wet summer monsoon in YRV. The belt of strong easterly wind anomalies centered around the Philippines that defines the southern boundary of the anticyclonic cell appears to propagate eastward after June. In October the easterly wind anomalies reach the equatorial eastern Pacific, which is consistent with the development of the observed cold SSTA there (Fig. 4 and Table 2).

The time scale of the apparent propagation of tropical anomalous easterly winds shown in Fig. 7 is quite slow compared with the atmospheric advective scale. Therefore, the propagation may result from atmosphere-ocean interaction. This interaction may involve the generation of atmosphere-ocean coupled Kelvin waves similar to those discussed by Hirst (1986). In this mechanism the interaction between the atmospheric surface wind and ocean thermocline leads to an unstable slow SSTA mode that has a Kelvin wave structure in both atmosphere and ocean fields and propagates eastward along the equator.

Since an interdecadal difference in the equatorial eastern Pacific SSTA is noticeable relative to the May-June YRV rainfall (Fig. 6), we will examine the wet-minus-dry 850 hPa wind composite sequence for the MJ season for both ID1 and ID2. The January to December time-longitude sections of this composite, averaged between equator and 15°N, for ID1 and ID2 are shown in Figs. 11a and 11b, respectively. The interdecadal difference in the equatorial eastern Pacific SSTA evolution relative to the YRV rainfall anomalies can be clearly related to the wind

composites. For ID1, anomalous easterlies appear east of the dateline starting in early spring. They soon strengthen and expand so that a wide longitudinal span covering both sides of the dateline is occupied by anomalous easterlies through summer and fall. This sequence of events is consistent with the cooling of the equatorial eastern Pacific in the northern spring before the wet YRV monsoon starts during ID1. In contrast, for ID2 (Fig. 11b) a belt of anomalous easterly winds first appears in June in the western Pacific and South China Sea. It then propagates slowly eastward and reaches the eastern Pacific in October. In a two-dimensional map (not shown) the belt starts as the southern edge of the anomalous anticyclonic cell that influences the YRV rainfall, and actually propagates slowly east-southeastward from the Philippine region to the equatorial eastern Pacific. This evolution is consistent with the delayed sign change of the equatorial eastern Pacific SSTA in northern fall of ID2.

In both interdecadal periods the evolution of the SSTA sign reversal in the equatorial eastern Pacific is associated with that of the anomalous easterly winds. Therefore, the difference in the timing of the SSTA sign reversal posts an interesting question on the possible mechanisms that differentiate the atmosphere-ocean interactions within the two periods. Fig. 12a shows the difference between the two wet composites of SST for March (ID2 wet composite minus ID1 wet composite). The interdecadal difference of a warmer SSTA in the tropical eastern Pacific that extends into the equatorial western Pacific, and a cooler region to its northwest that covers the midlatitude eastern Pacific and most of the tropical western Pacific, are clearly indicated. Fig. 12b shows the corresponding 850 hPa wind differences, where the central and eastern Pacific is dominated by westerly anomalies. A stronger westerly belt in the equatorial region is consistent with the warmer equatorial SST, and a separate belt of strong westerly winds to its north delineates a lower pressure center over the subtropical ocean. These patterns are consistent with the interdecadal mean differences observed by Zhang et al. (1997), who found the gross characteristics of the interdecadal variations similar to the ENSO variations.

The mechanisms that cause the interdecadal difference for the SSTA phase reversal are hypothesized as follows. The long-term mean equatorial eastern Pacific SST is several degrees below the threshold of that required for conditional instability. In addition, the low level easterly wind produces a mean divergence. Therefore, even under warm anomalies, it is difficult to sustain a positive feedback between zonal wind stress and zonally-asymmetric thermocline variations through the Walker cell-SSTA interaction<sup>4</sup>. In ID2 the mean equatorial eastern Pacific SST is nearly 1°K higher than in ID1 (Fig. 12a). Meanwhile, the warmer mean SST also produces a stronger mean low-level convergence, both due to zonal convergence along the equator (Fig. 12b) and meridional convergence due to the beta effect on the equatorial westerlies. During a warm phase within ID2 the combination of these two mean effects and the warm SSTA may be sufficient to elevate the environment to a favorable condition for convection. Therefore, the positive feedback between zonal wind stress and thermocline variations will be more likely to occur.

This interdecadal difference implies that a warm SSTA phase in ID1 may be much more likely to reverse its sign after the SSTA peak in northern winter, such as those observed in the TBO composites (e.g., Yasunari, 1990; Shen and Lau, 1995) and in the typical ENSO composites (e.g., Rasmusson and Carpenter, 1982). These composites all show a phase lock with the seasonal cycle such that the SSTA sign reversal occurs in northern spring (which has been termed the “boreal spring barrier” by Webster and Yang, 1992; Torrence and Webster, 1998, and others). Several theories have been proposed to explain this spring

---

<sup>4</sup> In this interaction warmer eastern Pacific SSTA enhance an anomalous Walker cell with increased surface westerlies, which further enhance the warm SSTA.

transition in ENSO. In Li's (1997) stationary SST mode theory, a seasonal cycle phase-locked negative feedback occurs through local Hadley cell and zonally-symmetric thermocline variations. In Wang et al. (2000) the negative feedback is due to ocean Kelvin waves generated by a western Pacific subtropical anticyclone which is primarily a Rossby wave response to the eastern Pacific SSTA. Both processes favor a peak of ENSO events in northern winter and a SSTA sign change a few months later. While a similar theory for more modest events such as the TBO has yet to emerge, the spring transition in ID1 has been considered normal in view of the large amount of observational results.

On the other hand, in ID2 the stronger positive Walker-thermocline feedback may overcome the seasonal cycle phase lock and sustain a warm phase beyond northern spring. In this case, when the anomalous anticyclone cell associated with a wet East Asian summer monsoon generates eastward-propagating anomalous easterly winds in the tropics through interactions with ocean or coupled Kelvin waves, the arrival of the easterly anomalies will help to cool the SST so that the transition occurs after northern summer, as indicated in Fig. 6. A similar cooling effect may not be easily detectable in ID1 since the equatorial wind anomalies have already reversed over a large longitudinal span before the summer monsoon.

## 5. Summary and Concluding Remarks

In this work (Part 1) the interannual relationship between the tropical Pacific SST and the East Asian summer monsoon is studied by compositing the SST, 500 hPa geopotential height and 850 hPa wind fields according to the 1951-1996 summer monsoon rainfall anomalies in the vicinity of the Yangtze River Valley. The data sets are also partitioned into two periods, 1951-77 and 1978-96, to study the possible interdecadal variations of this relationship. The major conclusions are summarized below:

1. A wet May-June monsoon in YRV is preceded by a warm equatorial eastern Pacific in the previous winter and followed by a cold equatorial eastern Pacific in the following fall. The relationship resembles a TBO pattern during the first interdecadal period of 1951-77 when the SSTA change sign in northern spring. In the second interdecadal period of 1978-96 the sign change occurs in northern fall and the TBO pattern in the equatorial eastern Pacific SST is replaced by longer time scales. These relationships are absent for the post-Meiyu (July - August) monsoon rainfall.
2. In a wet YRV monsoon year, the western North Pacific subtropical ridge is stronger as a result of the anomalous Hadley and Walker circulations and the complementary cooling in the western Pacific through an atmospheric Rossby wave response and the evaporation-wind feedback (Wang et al. 2000). The subtropical ridge also extends farther to the west from the previous winter to the following fall, resulting in an 850 hPa anomalous anticyclone near the southeast coast of China during spring and early summer. This anticyclone exerts three influences. First, it blocks the pre-Meiyu and Meiyu fronts from moving southward therefore extends the time the fronts stay stationary and produce rainfall. Second, it enhances the pressure gradient to its northwest resulting in a more intense Meiyu front. Third, it induces anomalous warming of the South China Sea surface through increased downwelling. The resultant warm SSTA provide higher moisture transport by the southwesterlies to the Meiyu rainfall area.
3. The cause of the interdecadal change of the SST-monsoon relationship is attributed to the change of interdecadal basic-state SST and wind changes in the Pacific. The growth rate of the coupled air-sea mode may depend strongly on the seasonal cycle basic state and it reaches a maximum in December (Li 1997). Afterwards, negative feedback processes (e.g., Battisti and Hirst, 1989, Li 1997, Wang et al. 2000) take over and may explain the spring phase transition of SSTA in the eastern Pacific during 1951-77. In 1978-96 the eastern

Pacific mean SST is higher. During a warm phase within this period the high SST, coupled with higher mean convergence near the surface, allows the development of positive feedback between the Walker cell and thermocline variations. The warm phase is therefore sustainable beyond northern spring.

4. There is evidence that the tropical anomalous easterly winds south of the spring and summer anomalous anticyclone propagate slowly eastward into the equatorial eastern Pacific after summer. We hypothesize that this is a result of monsoon-subtropical high interaction in which the western Pacific subtropical high near East Asia is reinforced to excite equatorial easterlies and a slow-propagating unstable air-sea mode (Hirst, 1986). These eastward-propagating coupled ocean-atmosphere Kelvin waves lead to a further cooling effect on the eastern Pacific SST after summer. This cooling effect is nearly non-discernible in 1951-77 because the SSTA phase transition has already taken place in northern spring. In 1978-96 the positive feedback between Walker cell and thermocline variations resists the negative feedback processes. The reversal of the SSTA sign occurs only when the eastward-propagating anomalous easterlies generated by the monsoon-subtropical ridge feedback arrive in northern fall and help to cool the SST.
5. The warming of the South China Sea surface, which may be at least partly due to the anomalous anticyclone in the spring and summer, appears in all wet seasons and the warm SSTA usually last through the monsoon season. This may explain Lau and Yang's (1997) findings that the development of the strong southwesterly monsoon over the South China Sea during the monsoon onset often foreshadows the development of the full-scale Asian monsoon during the entire summer, because the stronger pressure gradient near the western fringe of the anomalous anticyclone produces the strong southwesterlies and the sustained warm South China Sea SST is favorable for a strong monsoon.

The relationships between the East Asian summer monsoon and the eastern Pacific SSTA, in both the interannual and interdecadal scales, are mostly due to the variations of the western North Pacific subtropical ridge. The higher mean equatorial eastern Pacific SST in 1978-96 forces a stronger warm-phase anomalous anticyclone near the East Asian monsoon region than in 1951-77. This may also contribute to a stronger effect of the eastward-propagating tropical anomalous easterly winds in reversing the eastern Pacific SSTA in northern fall.

Our hypothesis that the anomalous anticyclone cell associated with a wet East Asian summer monsoon generates slow eastward-propagating air-sea coupled modes is similar to Wang et al.'s (2000) ENSO turnabout theory. The major difference is that the anticyclone in Wang et al. (2000) is related to ENSO and reaches its maximum intensity in northern winter. The anticyclone discussed here is associated with the anomalous East Asian summer monsoon. The rapid intensification of the anticyclone during the monsoon season implies that there may exist positive feedback between the subtropical high and the monsoon heating. Namely, a stronger subtropical ridge may increase the monsoon rainfall, which in turn may reinforce the ridge by enhancing the secondary circulation and subsidence over the subtropical high region. The exact process of the interaction remains an un-answered question and deserves further study

The similarity of the TBO pattern in the East Asian summer monsoon-eastern Pacific SST relationship with that in the Indian summer monsoon-eastern Pacific SST (e.g., Yasunari, 1990) does not mean that the East and South Asian summer monsoons are necessarily closely correlated themselves. It is possible that the eastern Pacific SSTs influence the East Asian summer monsoon through the subtropical ridge while influence the South Asian summer monsoon through a planetary scale east-west circulation. The cooling of the eastern Pacific

SST after spring may be a negative feedback process within the eastern Pacific not involving the monsoon, or a result of the anomalous east-west circulation associated with the South Asian monsoon as suggested by Chang and Li's (2000) TBO theory. In ID2 the monsoon-SST pattern becomes more complex due to the possible feedback from the East Asian summer monsoon through the West Pacific subtropical ridge, a process that does not involve the Indian monsoon.

We have concentrated on the relationship between monsoon rainfall and Pacific SST. The Indian Ocean SSTA tend to be in phase with the equatorial eastern Pacific and out-of-phase with the equatorial western Pacific. There have been suggestions in the Chinese literature that the moisture supply from the Bay of Bengal is an important source for the Meiyu rainfall (e.g., Ding, 1994). However, if this effect exists at the interannual scale it will be at least partially offset by the unfavorable 850 hPa wind anomalies in the Bay of Bengal, which are mostly directed away from the Meiyu area in the wet season composites (Fig. 7).

In this paper only the YRV monsoon in central China is studied. The question of the meridional phase structure of the East Asian monsoon will be addressed in Part 2, in which the relationship between the SEC rainfall and tropical SST will be discussed and compared with that of the YRV rainfall.

*Acknowledgments.* We wish to thank Prof. Haney for reading the manuscript. This work was supported by the National Science Foundation, under Grant ATM 9613746.

## References

- Battisti, D. S., and A. C. Hirst, 1989: Interannual variability in the tropical atmosphere-ocean system: Influence of the basic state, ocean geometry, and nonlinearity. *J. Atmos. Sci.*, **46**, 1687-1712.
- Chang, C.-P., and G. T. Chen, 1998: The development of an intense East Asian summer monsoon disturbance with strong vertical coupling. *Mon. Wea. Rev.*, **126**, 2692-2712.
- \_\_\_\_\_, and T. Li, 2000: A theory for the tropical biennial oscillation. *J. Atmos. Sci.*, in press.
- \_\_\_\_\_, Y. Zhang and T. Li, 1999: Interannual and Interdecadal Variations of the East Asian Summer Monsoon and the Tropical Sea-Surface Temperatures. Part 2: Southeast China Rainfall and Meridional Structure. *J. Climate*, submitted.
- Chen, G. T., and C.-P. Chang, 1980: Structure and Vorticity Budget of Early Summer Monsoon Trough (Mei-Yu) over Southeastern China and Japan. *Mon. Wea. Rev.*, **108**, 942-953.
- Chu, P. and C.-P. Chang, 1997: South China Sea warm pool in boreal spring. *Advances in Atmos. Sci.*, **14**, 195-206.
- \_\_\_\_\_, H. C. Tseng, C.-P. Chang and J. M. Chen, 1997: South China Sea warm pool detected in spring from the Navy's Master Oceanographic Observational Data Set (MOODS). *J. Geophys. Res.*, **102 C7**, 15761-15771.
- Ding, Y. H., 1992: Summer monsoon rainfalls in China. *J. Meteor. Soc. Japan*, **70**, 373-396
- \_\_\_\_\_, 1994: *Monsoon over China*, Kluwer Academic Publishers, 420pp.
- Hirst, A. C., 1986: Unstable and damped equatorial modes in simple coupled ocean-atmosphere models. *J. Atmos. Sci.*, **43**, 606-630.
- Huang, R. and Y. Wu, 1989: The influence of ENSO on the summer climate change in China and its mechanism. *Advances in Atmos. Sci.*, **6**, 21-32.
- \_\_\_\_\_, and F. Sun, 1992: Impacts of the tropical western Pacific on the East Asian summer monsoon. *J. Meteor. Soc. Japan*, **70**, 243-256.
- Johnson, R. H., Z. Wang, and J. F. Bresch, 1993: Heat and moisture budgets over China during the early summer monsoon. *J. Meteor. Soc. Japan*, **71**, 137-152.
- Lau, K. M., and S. Yang, 1996: The Asian monsoon and predictability of the tropical ocean-atmosphere system. *Q. J. Roy. Meteorol. Soc.*, **122**, 945-957.
- \_\_\_\_\_, and \_\_\_\_\_, 1997: Climatology and interannual variability of the Southeast Asian summer monsoon. *Advances in Atmos. Sci.*, **14**, 141-162.
- \_\_\_\_\_, and H. Weng, 1999: Interannual, decadal-to-interdecadal and global warming signals in sea surface temperature during 1955-1997. *J. Climate*, **12**, 1257-1267.
- Li, T., 1997: Phase transition of the El Nino-Southern Oscillation: A stationary SST mode. *J. Atmos. Sci.*, **54**, 2872-2887.
- Liu, Y. and Ding, Y. H., 1992: Influence of El Nino on weather and Climate in China. *Acta meteorological Sinica*, **6(1)**, 117-131
- Meehl, G. A., 1987: The annual cycle and interannual variability in the tropical Pacific and Indian Ocean region. *Mon. Wea. Rev.*, **115**, 27-50.
- \_\_\_\_\_, 1997: The South Asian monsoon and the tropospheric biennial oscillation (TBO). *J. Climate*, **10**, 1921-1943.
- \_\_\_\_\_, and W. M. Washington, 1996: El Nino-like climate change in a model with increased atmospheric CO<sub>2</sub> concentrations. *Nature*, **382**, 56-60.
- Nitta, T., and S. Yamada, 1989: Recent warming of tropical sea surface temperature and atmospheric flow patterns. *J. Meteor. Soc. Japan*, **67**, 375-383.
- \_\_\_\_\_, and Z. Z. Hu, 1996: Summer climate variability in China and its association with 500 hPa height and tropical convection. *J. Meteor. Soc. Japan*, **74**, 425-445.
- Rasmusson, E. M., and T. H. Carpenter, 1982: Variations in the tropical sea surface temperature and surface wind fields associated with the Southern Oscillation/El Nino. *Mon. Wea. Rev.*, **110**, 354-384.

- Shen, S., and K. M. Lau, 1995: Biennial oscillation associated with the east Asian monsoon and tropical sea surface temperatures. *J. Meteor. Soc. Japan*, **73**, 105-124.
- Tanaka, M., 1997: Interannual and interdecadal variations of the western North Pacific monsoon and Baiu rainfall and their relationship to the ENSO cycle. *J. Meteor. Soc. Japan*, **75**, 1109-1123.
- Tao, S.Y. and L. X. Chen, 1987: : A review of recent research of the East Asian summer monsoon in China. *Monsoon Meteorology*, C.-P. Chang and T. N. Krishnamurti, Eds., Oxford University Press, 60-92.
- Tian S. F. and T. Yasunari, 1992: Time and space structure of interannual variations in summer rainfall over China. *J. Meteor. Soc. Japan*, **70**, 585-596.
- Trenberth, K. E., and Hurrell, 1994: Decadal atmosphere-ocean variations in the Pacific. *Climate Dynamics*, **9**, 303-319.
- \_\_\_\_\_, and T. J. Hoar, 1996: The 1990-1995 El Nino-Southern Oscillation event: Longest on record. *Geophys. Res. Lett.*, **23**, 57-60.
- Torrence, C. and P. J. Webster, 1998. The annual cycle of persistence in the El Nino/Southern Oscillation. *Quar. J. Roy. Meteor. Soc.*, **124**, 1985-2004.
- Wang, B., 1995: Interdecadal changes in El Nino onset in the last four decades. *J. Climate*, **8**, 267-285.
- \_\_\_\_\_, R. Wu, and R. Lukas, 2000: A new paradigm for ENSO turnabout. . *J. Climate*, **13**, in press.
- Webster, P. J., V. O. Magana, T. N. Palmer, J. Shukla, R. A. Tomas, M. Yanai, and T. Yasunari, 1998: Monsoons: Processes, predictability, and the prospects for prediction. *J. Geophys. Res.*, **103-C7**, 14451-14510.
- \_\_\_\_\_, and S. Yang, 1992: Monsoon and ENSO: Selectively interactive systems. *Quar. J. Roy. Meteor. Soc.*, **118**, 877-926.
- Weng, H., K-M. Lau and Y. Xue, 1999: Multi-scale summer rainfall variability over China and its long-term link to global sea surface temperature variability. *J. Meteor. Soc. Japan*, **77**, 845-857.
- Yasunari, T., 1990: Impact of Indian monsoon on the coupled atmosphere/ocean system in the tropical Pacific. *Meteo. Atmos. Phys.*, **44**, 29-41.
- \_\_\_\_\_, 1991: The monsoon year – a new concept of the climate year in the tropics. *Bull. Amer. Meteor. Soc.*, **72**, 1331-1338.
- Yatagai A., and T. Yasunari 1995: Interannual variations of summer precipitation in the arid/semi-arid regions in China and Mongolia: their regionality and relationship to the Asian monsoon. *J. Meteor. Soc. Japan*, **73**, 909-923.
- Zhang, Y., J. M. Wallace, and D. S. Battisti, 1997: ENSO-like interdecadal variability: 1900-1993. *J. Climate*, **10**, 1004-1020.

Table 1. Categorization of rainfall in the YRV region.  
 1: very wet, 2: wet, 3: normal, 4: dry, 5: very dry.

YRV year	MJJA			MJ			JA		
	ALL	ID1	ID2	ALL	ID1	ID2	ALL	ID1	ID2
1951	3	3	-	5	4	-	2	2	-
1952	2	2	-	3	3	-	1	2	-
1953	4	4	-	3	3	-	4	4	-
1954	1	2	-	1	2	-	1	2	-
1955	3	3	-	2	2	-	4	3	-
1956	1	2	-	1	2	-	3	3	-
1957	3	3	-	4	4	-	3	3	-
1958	3	3	-	4	4	-	3	3	-
1959	4	4	-	1	2	-	5	4	-
1960	4	4	-	3	3	-	4	4	-
1961	5	4	-	4	4	-	4	4	-
1962	2	2	-	3	3	-	1	2	-
1963	3	3	-	4	4	-	2	2	-
1964	4	3	-	2	3	-	5	4	-
1965	3	3	-	5	4	-	1	2	-
1966	5	4	-	5	4	-	5	4	-
1967	4	4	-	2	3	-	5	4	-
1968	3	3	-	5	4	-	2	2	-
1969	1	2	-	3	3	-	1	2	-
1970	2	2	-	2	2	-	3	3	-
1971	4	4	-	2	2	-	5	4	-
1972	4	4	-	4	4	-	3	3	-
1973	1	2	-	1	2	-	3	3	-
1974	3	3	-	3	3	-	3	3	-
1975	2	2	-	2	2	-	3	2	-
1976	5	4	-	3	3	-	5	4	-
1977	2	2	-	1	2	-	3	3	-
1978	5	-	4	5	-	4	5	-	4
1979	4	-	4	3	-	3	4	-	4
1980	1	-	2	2	-	2	1	-	2
1981	5	-	4	5	-	4	3	-	3
1982	3	-	3	4	-	4	1	-	2
1983	1	-	2	2	-	2	2	-	2
1984	3	-	3	3	-	3	3	-	3
1985	5	-	4	5	-	4	4	-	4
1986	5	-	4	4	-	4	4	-	4
1987	3	-	3	4	-	4	2	-	2
1988	3	-	3	3	-	3	3	-	3
1989	2	-	2	3	-	2	2	-	2
1990	3	-	3	3	-	3	3	-	3
1991	2	-	2	2	-	2	2	-	3
1992	3	-	3	4	-	3	3	-	3
1993	1	-	2	1	-	2	2	-	2
1994	4	-	4	3	-	3	4	-	4
1995	2	-	2	1	-	2	4	-	4
1996	2	-	3	3	-	3	2	-	3

Table 2. Correspondence between equatorial eastern Pacific SSTA and YRV rainfall anomalies. +, −, and 0 mean the SSTA corresponding to a wet season are warm, cold, and small, respectively. Thick boundary lines enclose the columns of the rain season.

EEP	Dec	Jan	Feb	Mar	Apr	May	Jun	Jul	Aug	Sep	Oct	Nov
ALL	+	+	+	+	+	+	+	0	0	0	-	-
51-77(ID1)	++	++	++	0+	--	-0	--	-0	--	-0	-0	-0
78-96(ID2)	+0	++	++	++	++	++	++	++	++	00	00	-0
ALL MJ	+	+	+	0	0	0	0	-	-	-	-	-
51-77 MJ	++	++	0+	-0	--	--	--	--	--	--	--	--
78-96 MJ	++	++	++	++	++	++	++	++	0+	--	--	-0
ALL JA	+	+	+	+	0	+	+	0	+	+	+	+
51-77 JA	0+	00	00	00	00	++	+0	+0	++	++	++	++
78-96 JA	++	++	++	++	++	++	++	++	++	++	++	++

Table 3. Correspondence between South China Sea SSTA and YRV rainfall anomalies. +, −, and 0 mean the SSTA corresponding to a wet season are warm, cold, and small, respectively. Thick boundary lines enclose the columns of the rain season.

SCS	Dec	Jan	Feb	Mar	Apr	May	Jun	Jul	Aug	Sep	Oct	Nov
ALL	0	+	0	0	0	+	+	+	+	+	+	-
51-77(ID1)	00	++	00	00	+0	++	++	++	++	00	+0	--
78-96(ID2)	00	++	--	00	0-	-0	++	++	++	++	++	++
ALL MJ	+	+	0	0	0	+	+	+	+	0	0	-
51-77 MJ	00	++	++	+0	+0	++	++	++	+0	+0	--	--
78-96 MJ	00	++	-0	0-	00	-0	++	++	++	++	00	00
ALL JA	0	0	0	0	0	+	+	0	+	+	+	+
51-77 JA	-0	0+	--	-0	--	++	++	00	00	00	++	00
78-96 JA	-0	--	--	00	--	0-	+0	+0	++	++	++	++

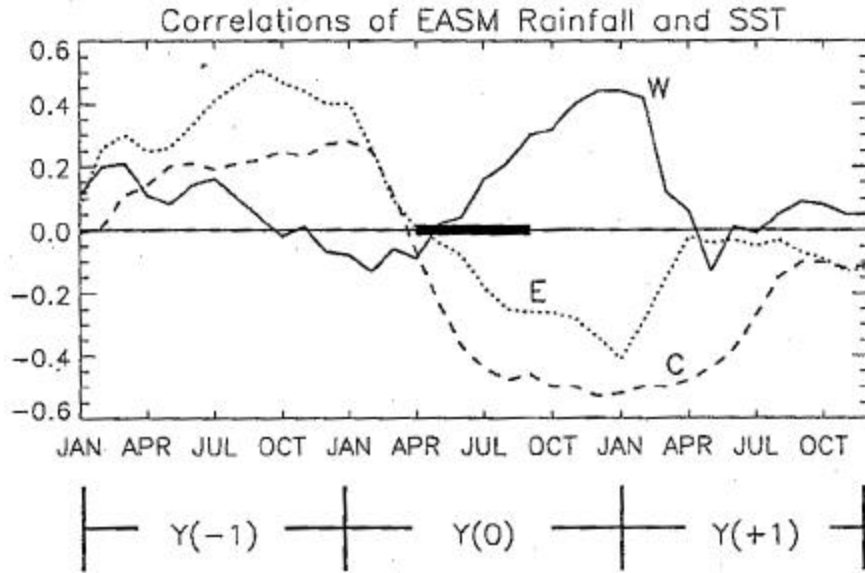


Fig. 1. Lagged correlations between the East Asian summer monsoon rainfall anomaly and the SST anomaly in the western Pacific Ocean ( $120^{\circ}\text{E}$ - $140^{\circ}\text{E}$ ,  $0^{\circ}$ - $8^{\circ}\text{N}$ , solid), the central Pacific ( $170^{\circ}\text{W}$ - $150^{\circ}\text{W}$ ,  $0^{\circ}$ - $8^{\circ}\text{N}$ , long dashed) and the eastern Pacific ( $90^{\circ}\text{W}$ - $82^{\circ}\text{W}$ ,  $10^{\circ}\text{S}$ - $0^{\circ}$ , short dashed), computed by Shen and Lau (1995) using the 1956-1985 data. Y(-1) and Y(+1) refer to the year before and after the reference year (Y0). The April-September rainfall season is marked by a horizontal bar Adopted from Fig. 9 of Shen and Lau (1995).

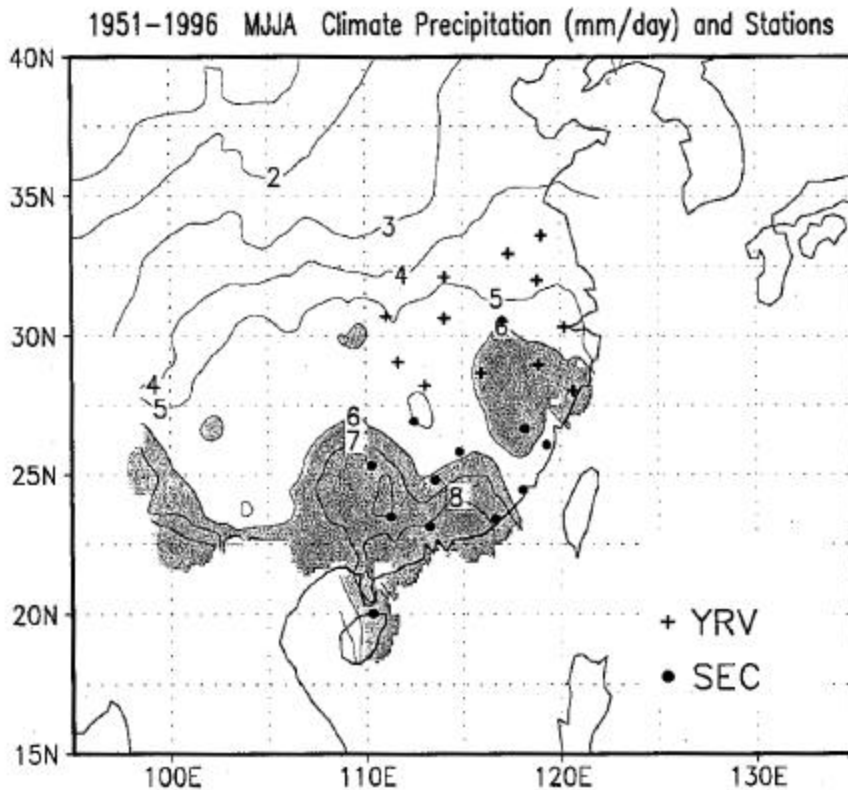


Fig. 2. Rainfall stations in the Yangtze River Valley (YRV) and the southeastern coastal area of China (SEC), superimposed with the 1951-1996 averaged summer (May-August) rainfall pattern.

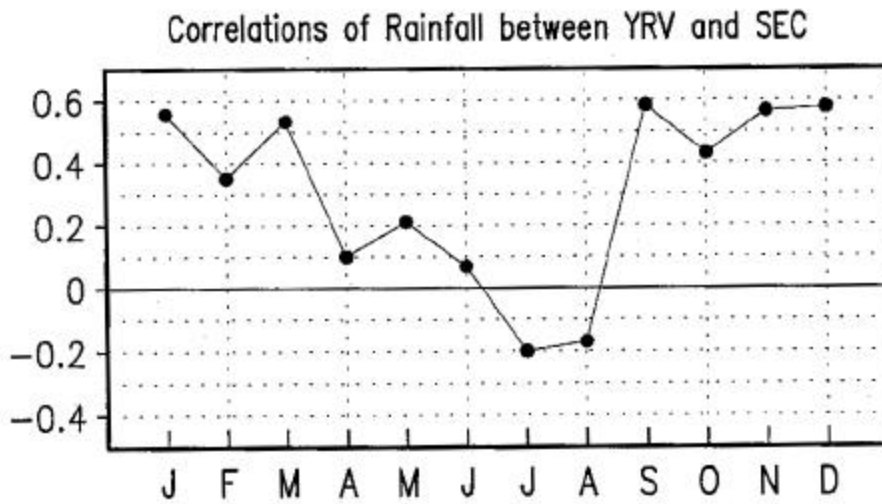


Fig. 3. Annual distribution of the correlations of monthly rainfall between the Yangtze River Valley and the southeastern coastal area of China for the 46-year data.

## YRV Index (1951–96), MJJA

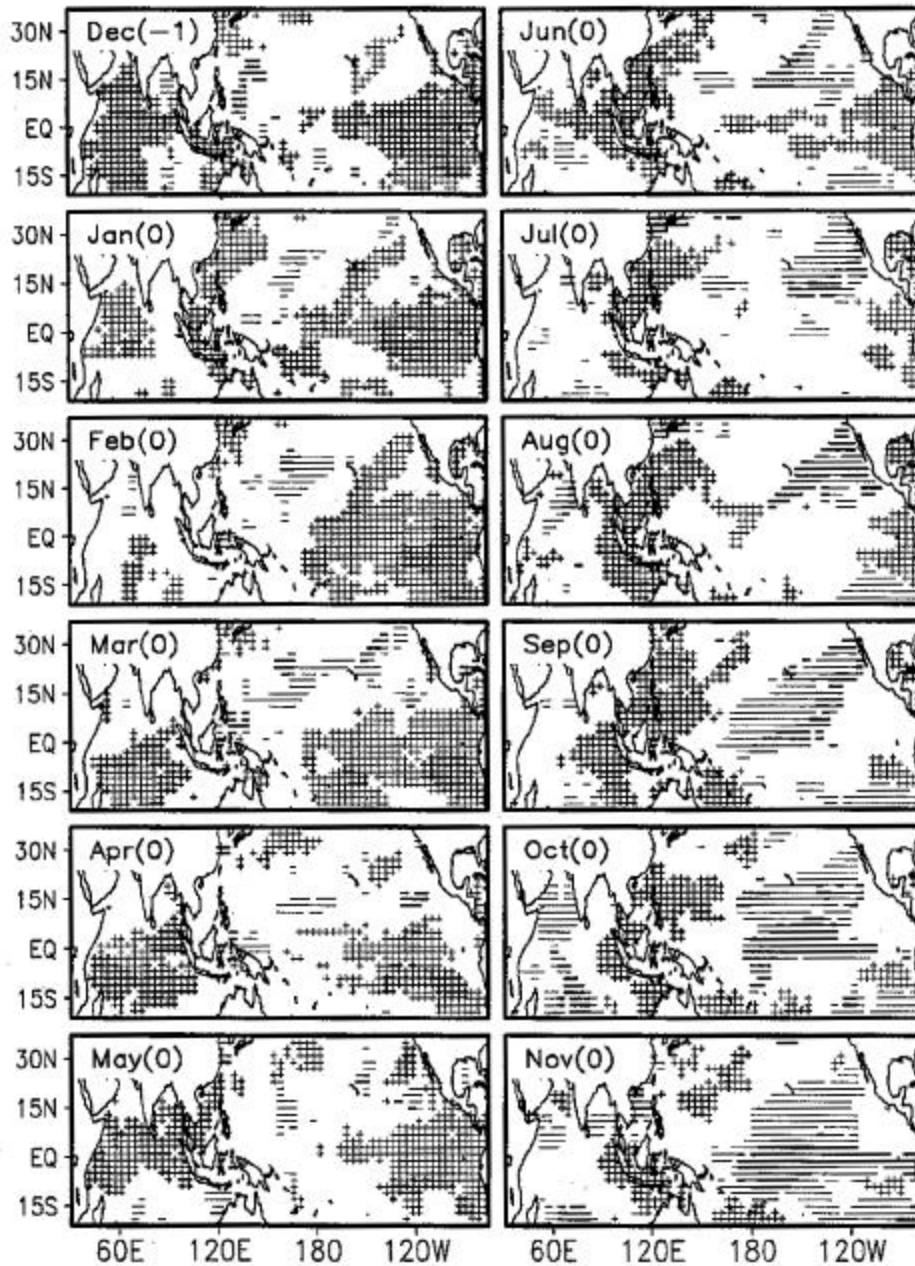


Fig. 4. The composite relationship between monthly SSTA, from December before the monsoon season to November after the monsoon, and the all-summer YRV monsoon rainfall anomalies, for the 46-year data set. **+**: SSTA positive for both very wet and wet, and negative for both very dry and dry; **+**: SSTA positive for very wet and negative for very dry, and either very wet in-phase with wet or very dry in-phase with dry but not both; **-**: SSTA negative for both very wet and wet, positive for both very dry and dry; **-**: SSTA negative for very wet and positive for very dry, and either very wet in-phase with wet or very dry in-phase with dry but not both. See text for details.

## YRV Index (1951–77), MJJA

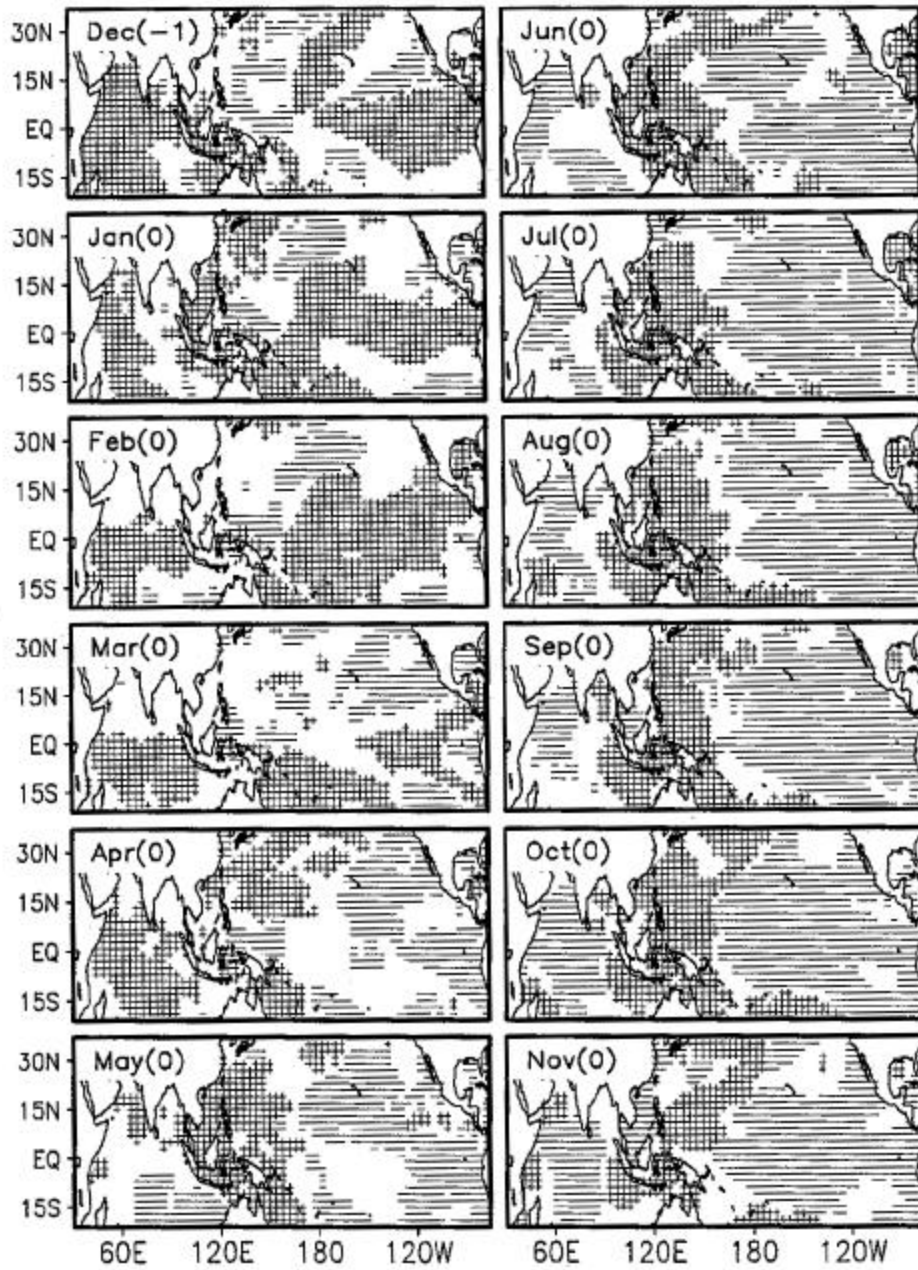


Fig. 5a. Same as Fig. 4 except for the ID1 period (1951-77) and the SSTA are departures from the ID1 period mean. These are referred to as the "intra-period relationship" for the interdecadal period in text. Also, the monsoon rainfall is classified into only three categories, with + indicating SSTA and monsoon rainfall anomalies are of the same sign and - indicating opposite sign.

### YRV Index (1978-96), MJJA

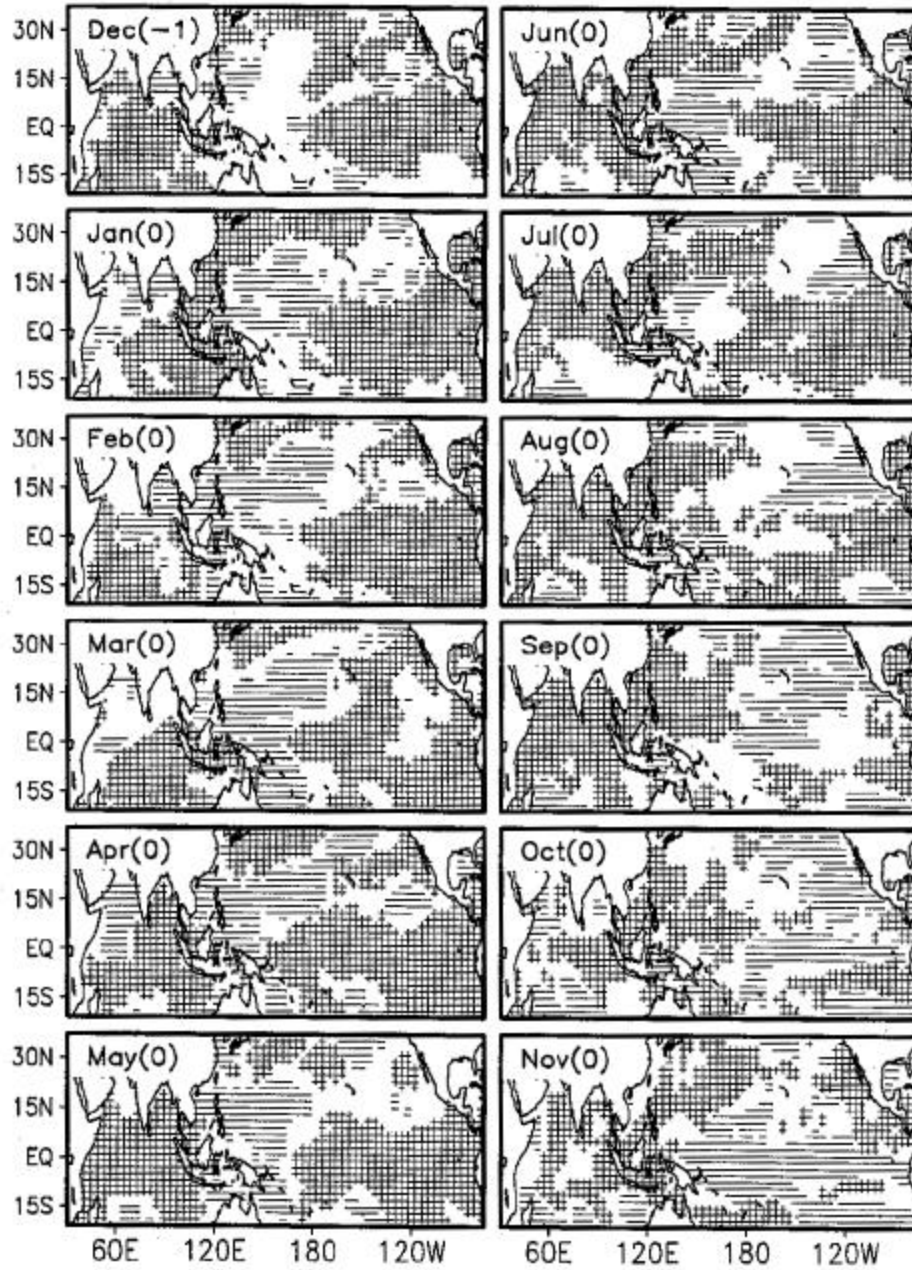


Fig. 5b. Same as Fig. 5a except for the ID2 period (1978-96) and the SSTA are departures from the ID2 period mean.

SST Composite (Wet Minus Dry, MJJA) over E. Pacific

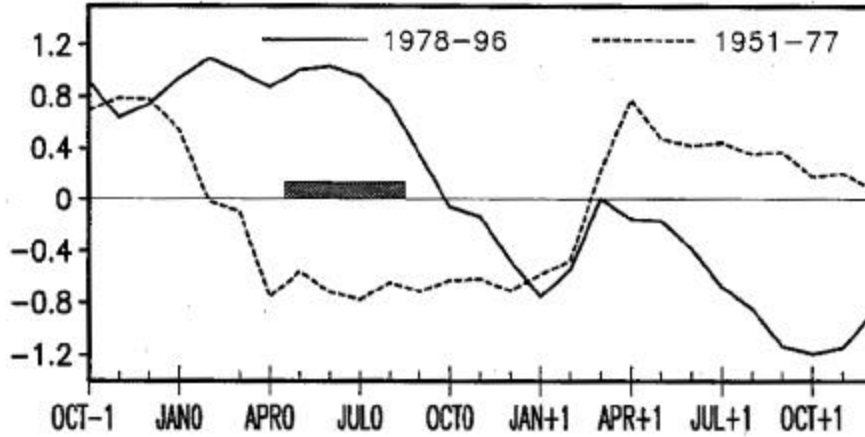


Fig. 6. The wet-minus-dry SST from October before the monsoon to October after the monsoon in the equatorial eastern Pacific ( $105^{\circ}\text{W}$ - $85^{\circ}\text{W}$ ,  $5^{\circ}\text{S}$ - $5^{\circ}\text{N}$ ) for ID1 (dashed) and ID2 (solid). The May-August monsoon rainfall season is marked by a horizontal bar.

YRV (1951-96), MJJA  $\vec{S}$  (m/s)

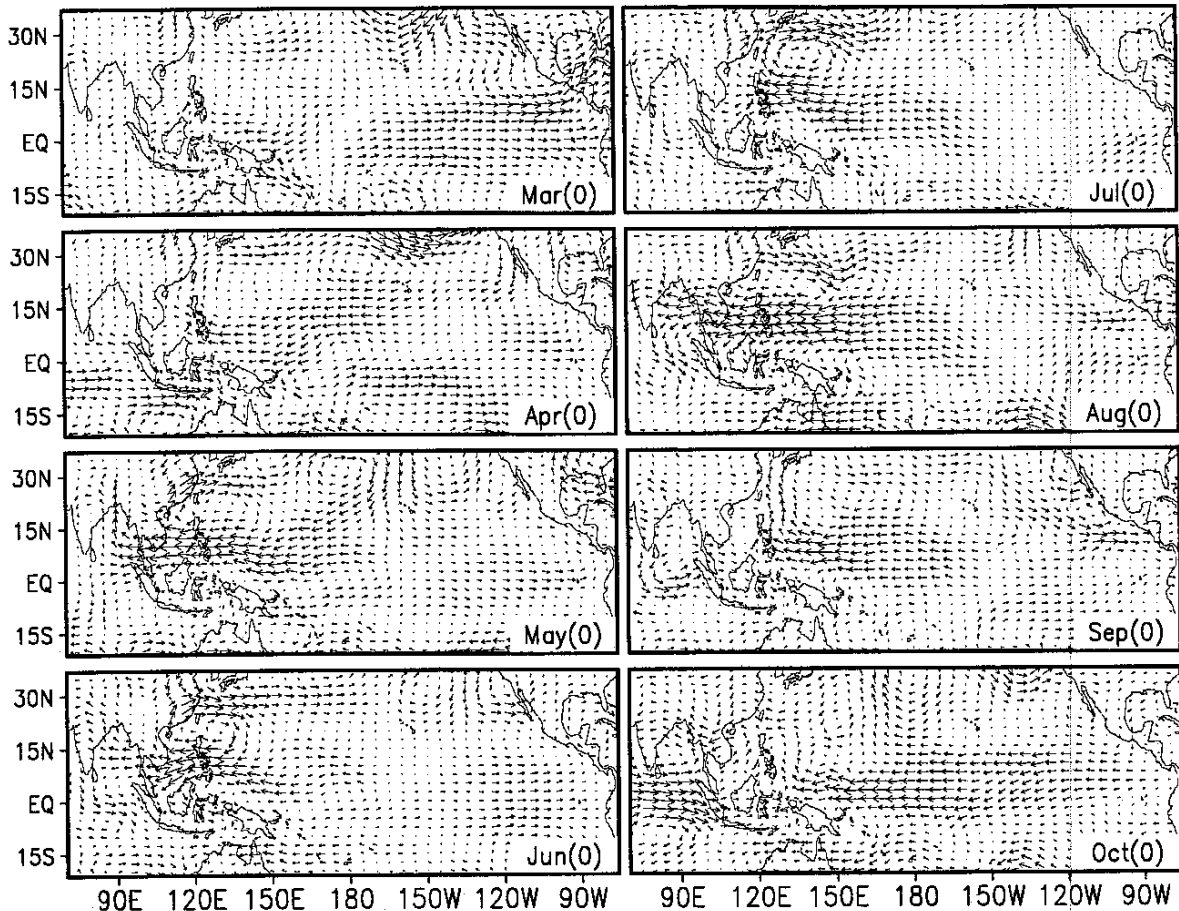


Fig. 7. Wet-minus-dry composite of the 850 hPa wind differences ( $\text{m s}^{-1}$ ), from March before the monsoon season to October after the monsoon, as computed from the all-summer YRV monsoon rainfall anomalies for the 46-year data set.

500hPa YRV (1951-96), MJJA

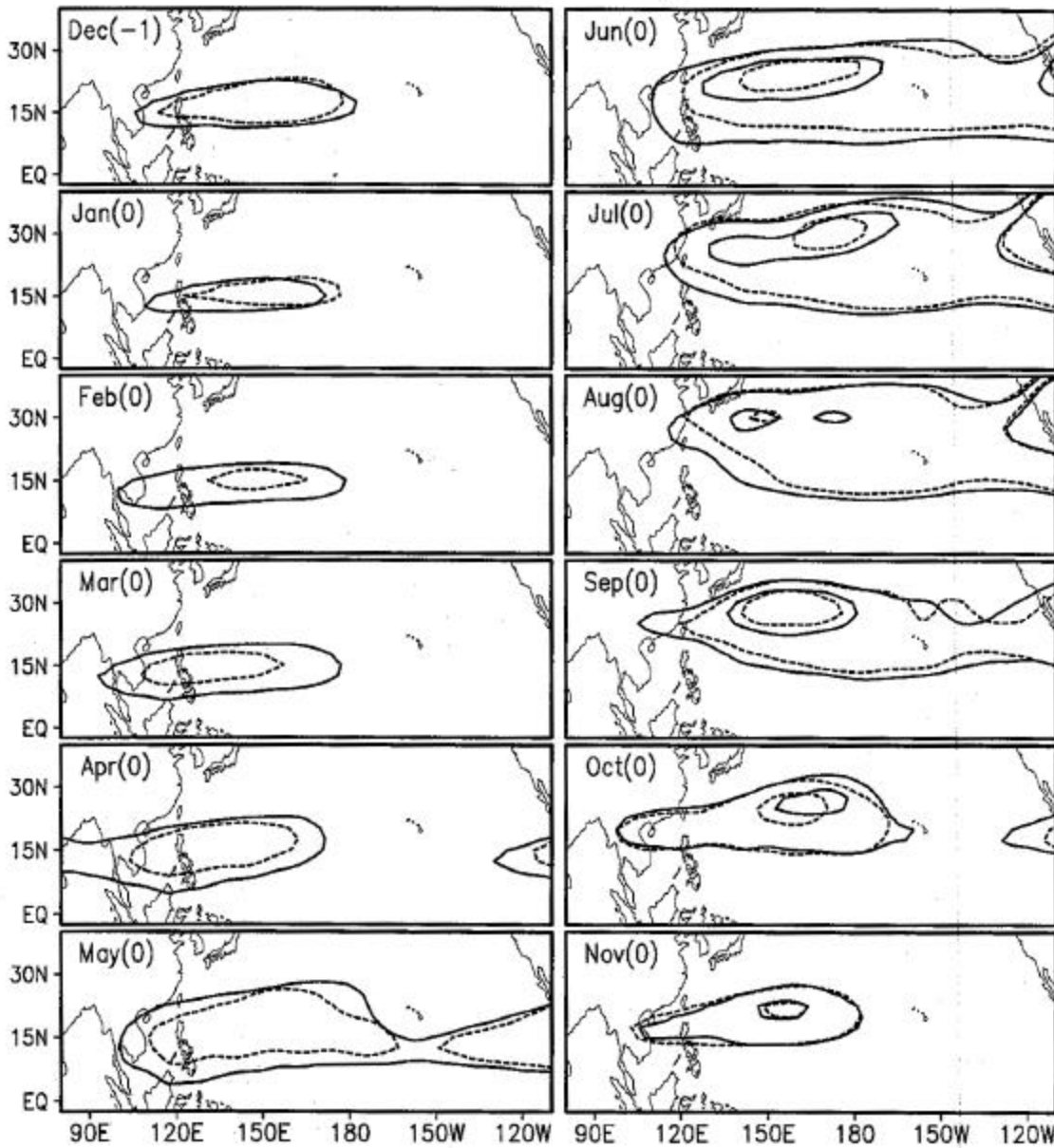


Fig. 8. The composite monthly 500 hPa geopotential height, indicated by the 5860 m and 5880 m contours, from December before the monsoon season to November after the monsoon for wet (solid) and dry (dashed) categories as computed from the all-summer YRV monsoon rainfall anomalies for the 46-year data set.

500hPa YRV (1951-96), MJJA Unit: 10gpm

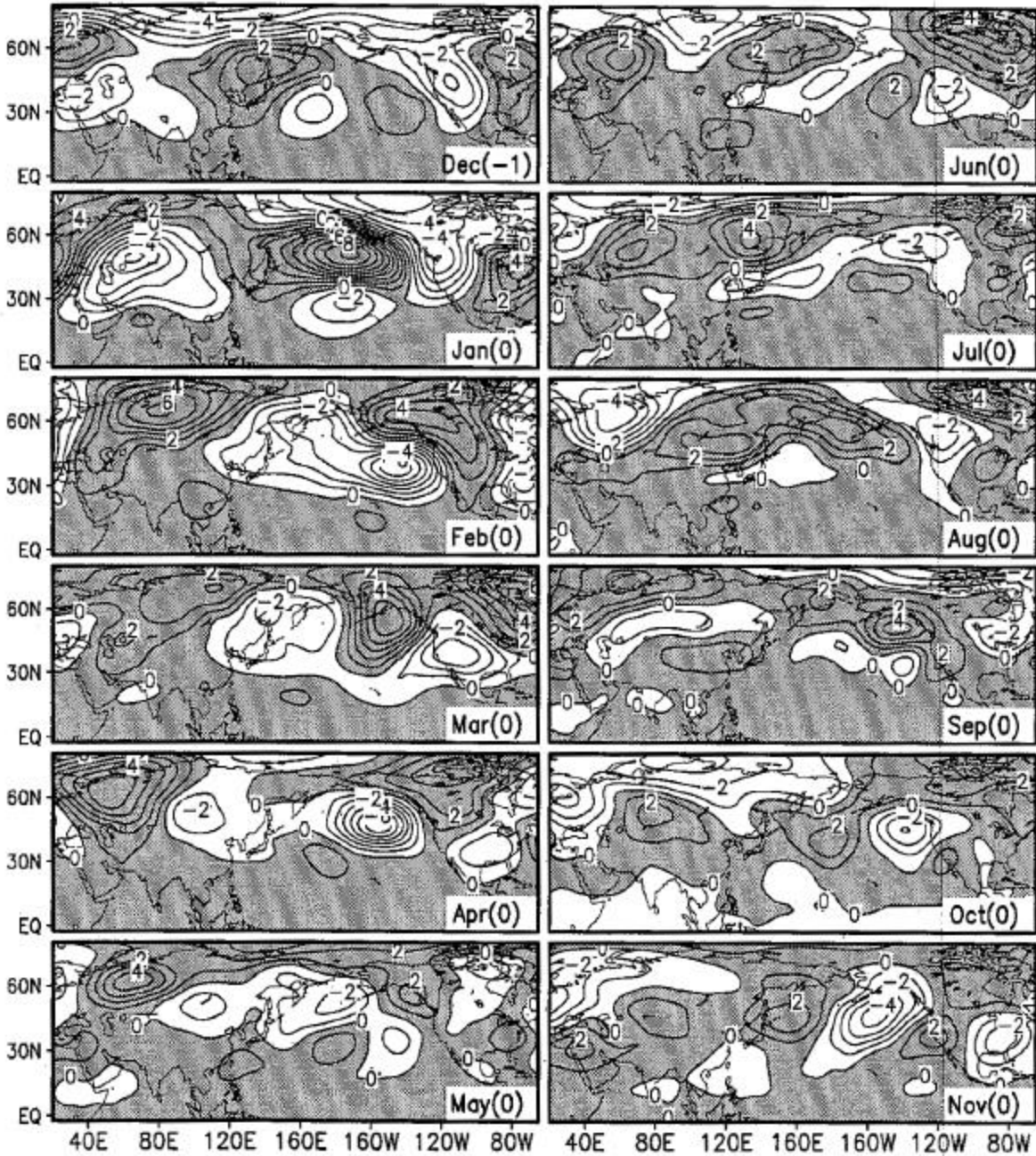


Fig. 9. Wet-minus-dry composite of the 500 hPa height (10 m), from December before the monsoon season to November after the monsoon, as computed from the all-summer YRV monsoon rainfall anomalies for the 46-year data set.

500hPa YRV (1951-77), MJ

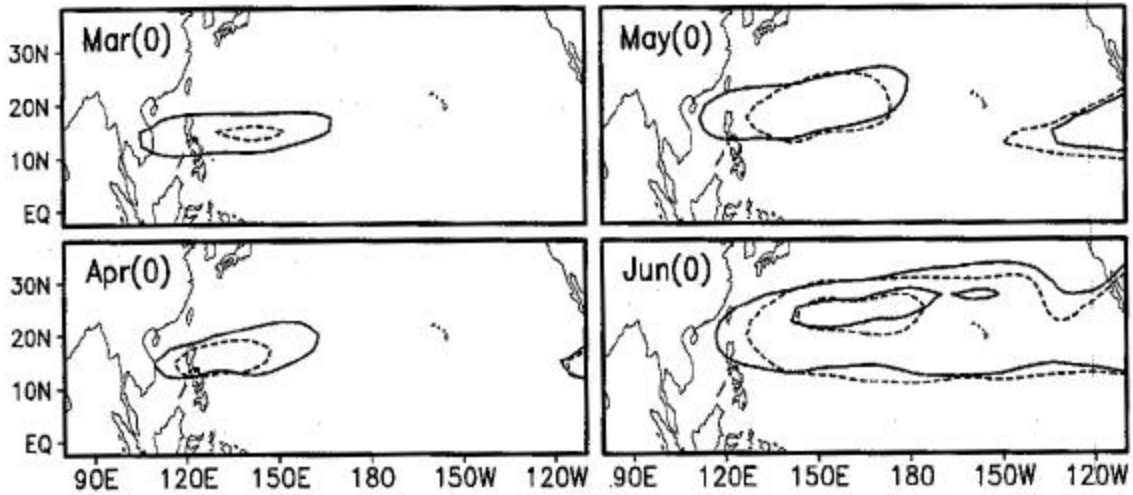


Fig. 10a. The composite monthly 500 hPa geopotential height, indicated by the 5860 m and 5880 m contours, from March before the monsoon season to June after the monsoon for wet (solid) and dry (dashed) categories as computed from the May-June YRV monsoon rainfall anomalies for the ID1 period.

500hPa YRV (1978-96), MJ

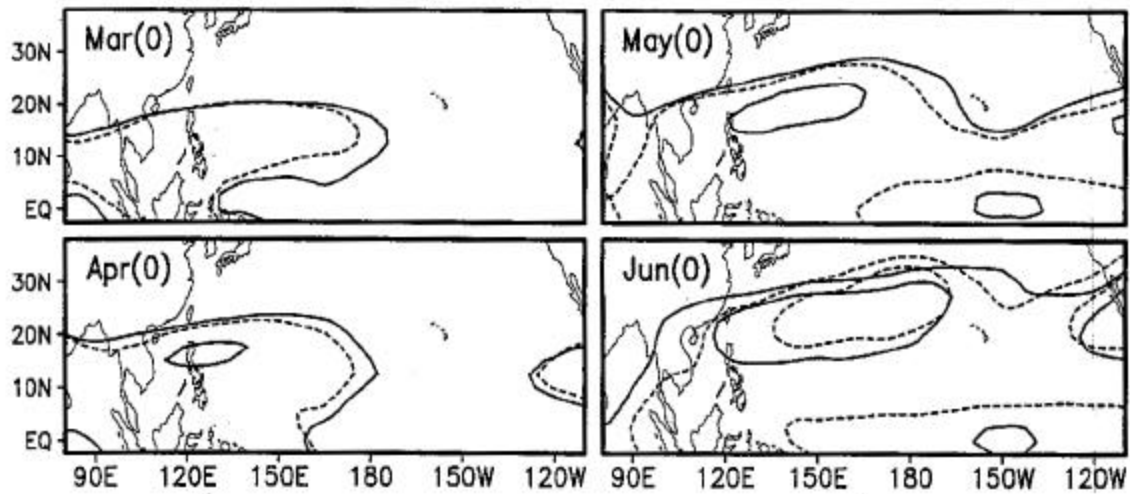


Fig. 10b. Same as Fig. 10a except for the ID2 period.

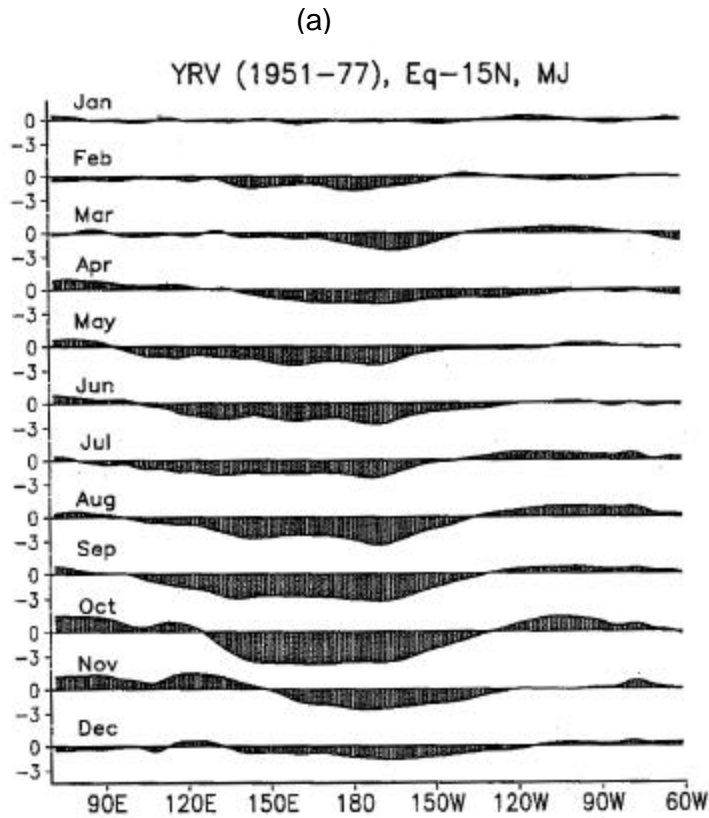


Fig. 11a. Time-longitude section of the wet-minus-dry composite (based on MJ rainfall anomalies) of the 850 hPa wind differences ( $\text{m s}^{-1}$ ), averaged between equator and  $15^\circ\text{N}$ , for the ID1 period.

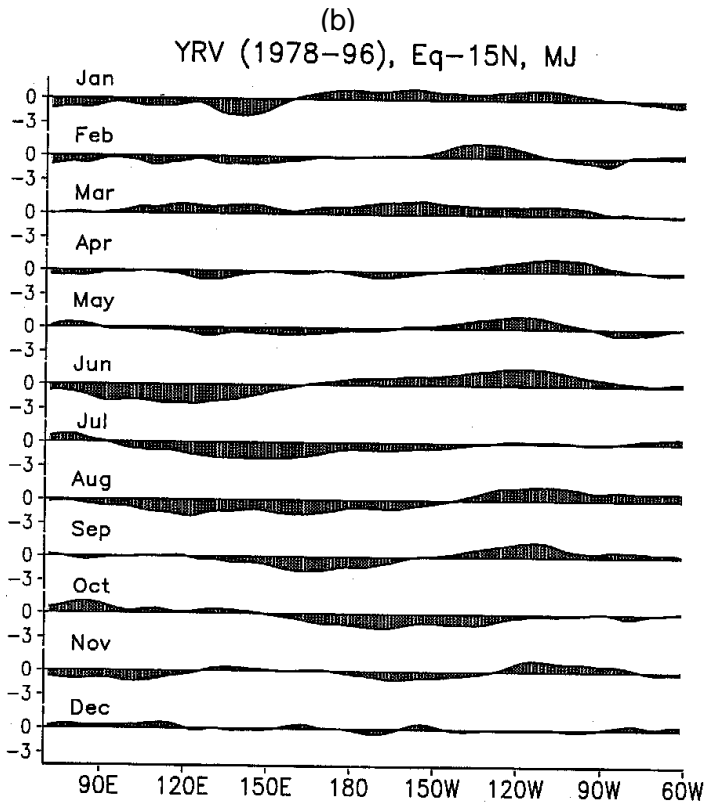


Fig. 11b. Same as Fig. 11a except for the ID2 period.

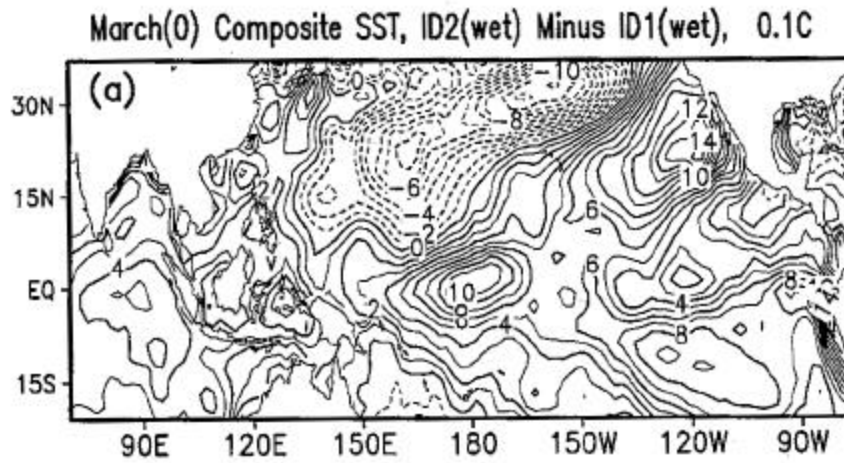


Fig. 12a. Interdecadal SST differences for March (ID2 wet composite minus ID1 wet composite).

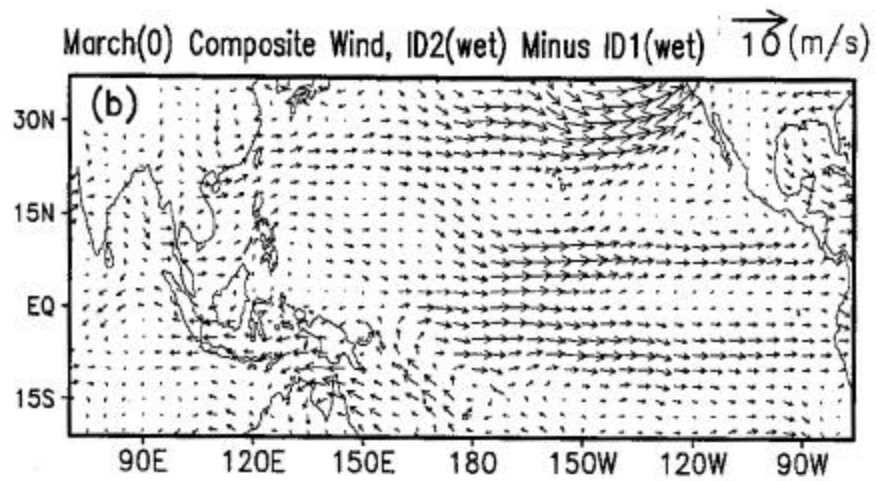


Fig. 12b. Same as Fig. 12a except for the 850 hPa wind differences.